https://doi.org/10.3311/PPee.21181

Periodica Polytechnica Electrical Engineering and Computer Science, 67(3), pp. 291–299, 2023

Piano Soundboard Analysis at Radiated Sound

Dóra Jenei-Kulcsár[1*], Péter Fiala[1]

[1] Department of Networked Systems and Services, Faculty of Electrical Engineering and Informatics, Budapest University of Technology and Economics, Műegyetem rkp. 3., H-1111 Budapest, Hungary
[*] Corresponding author, e-mail: dkulcsar@hit.bme.hu

Received: 15 September 2022, Accepted: 31 January 2023, Published online: 18 April 2023

Abstract

The piano is a complex musical instrument consisting of several components influencing vibration and sound production. By understanding the sound production mechanism virtual instruments can be created (physics-based sound synthesis) and the design and manufacturing of soundboards can be supported (virtual prototyping). Based on previous results published in the literature, a piano model was built and extended by a near field sound radiation model capable for physics-based sound synthesis. In this paper a simplified piano model is presented, including hammer strike and hysteretic felt models, coupled lossy string model and a 2D FEM based stiffened plate model for soundboard. This paper contains a parametric study where the soundboard parameters, such as its material characteristics and boundary conditions, are modified and their effect on the soundboard's modal behavior and the radiated sound is analyzed. Instead of using only musical (qualitative) descriptors, e.g. brightness or coloring, the piano sounds are characterized based on standard quantitative descriptors (e.g. harmonic ratio, spectral centroid). It is shown that these descriptors are determined by soundboard admittance, string characteristics and position on the soundboard; radiated sound from wooden soundboards can be characterized as harmonic for wide range of initial material descriptors; the string position is essential, and the perceived sound can differ significantly for different listening positions, even for the same harmonic decay pattern.

Keywords

piano modeling, piano soundboard, physics-based sound synthesis, quantitative descriptors of piano tone

1 Introduction

Mechanical and acoustic modeling of the piano has been of great interest for more than a hundred years due to the variety of elements from strike to sound radiation. Besides the hammer action and strings, soundboards are amongst the most widely modelled parts in the sound production chain. Their geometry and material properties affect the sound quality through inter-string coupling and sound radiation mechanism. By understanding the sound production mechanism development and manufacturing of traditional and experimental soundboards can be supported (virtual prototyping e.g. [1]) and virtual instruments (e.g. [2]) can be created.

Piano soundboards are complex structures where the main resonator (plate) is stiffened and slightly bent with ribs on the bottom, while on the upper side bridges are installed. The main resonator is traditionally built from solid music wood.

The modal behavior of the piano soundboard and its influence on tone quality has widely been examined (e.g. [3–7]). It is mostly modelled based on numerical abstractions (e.g. [8–14]), but some research for (semi)analytical solutions also exists (e.g. [5, 15–17]).

The published and widely used material characteristics, frequency response and vibrational properties for wood materials are outputs of measurements and structural models (e.g. [18–24]). Wood choice for instruments manufacturing is also affected by geo-cultural and economic motives (e.g. [25, 26]), resulting in traditional wood species for given instruments. Based on this information, wood properties for piano models can be determined (e.g. [10, 27, 28]).

To be able to study the soundboard, the present research applies a reduced model of the piano that covers the sound production chain from hammer strike to the radiated sound. Different elements of the system are modelled using diverse (1D, 2D, 3D) approaches. The piano hammer's wooden core, covered by multi-layer felt, is mostly modeled as elastic and hysteretic spring [29]. Piano strings are made of piano wire, which is a tempered high-carbon steel wire having very high tensile strength. The motion of

Cite this article as: Jenei-Kulcsár, D., Fiala, P. "Piano Soundboard Analysis at Radiated Sound", Periodica Polytechnica Electrical Engineering and Computer Science, 67(3), pp. 291–299, 2023. https://doi.org/10.3311/PPee.21181

excited strings is complex, but Smith [30] has shown that these can be successfully modelled by digital waveguides. Bank [31] improved the excitation model so that it can be properly applied for the struck strings.

The piano sound is radiated by the soundboard into the surrounding acoustic field. Without modeling the room around the instruments, resulting sound can be considered by a near field sound radiation model, neglecting multipath propagation and acoustic short circuits. This simple model is appropriate to analyze the impact of the piano soundboard on the radiated sound.

This paper, besides a brief piano model overview, presents a finite element model of the traditional piano soundboard. The material model is based on the generalized Hooke's law valid for orthotropic materials. The resulting equation of forces and moments is derived from the Kirchhoff-Love thin plate theory. The numerical model of the geometry is based on the finite element approach, applying the master-slave concept in ribbed case.

Our modeling objective is to determine the modal behavior of this structure: how is it affected by the parameter selection, and how does it influence the resulting sound. Based on eigenfrequencies, mode shapes and modal damping coefficients it is possible to consider the modelled piano soundboard as terminator and coupling element in the string model and as acoustical radiator for near field sound synthesis. In both cases predefined filter sets can be parametrized and applied using the modal description.

In the current study on the impact of modifying the initial mechanical and geometrical parameters is not only assessed through the investigation of the soundboard's modes, but also on the produced near field piano sound. Piano tone is characterized using standard quantitative indicators (as decay, harmonic ratio, loudness, spectral slope, flux and centroid), instead of qualitative effective parameters, influenced by psycho-acoustical effects (as e.g. brightness, pleasingness and coloring).

In the next sections we briefly introduce the developed model and present some simulation results based on a simplified but quasi-realistic piano model.

2 The soundboard model in the piano model

2.1 Piano model overview

The piano model is limited to the hammer-string-soundboard interaction, terminated by the near field sound radiation model.

2.1.1 The hammer felt model

The input force created by the piano hammer as a function of actual displacements is well defined by the second law of Newton

$$F_h = m_h \cdot \frac{\partial^2 u_h}{\partial t^2}, \tag{1}$$

where F_h is the total hammer force ($F_h = \sum_k F_f^k$, where k is the number of struck strings) acting on strings, m_h is the mass of the hammer head and u_h is the actual displacement of the hammer.

The felt force can accurately be modelled as a hysteretic spring. The elastic (F_f^{el}) and dissipative (F_f^{dis}) parts of the acting force are additive [27]. While the elastic part is described by the elastic force model, different dissipative force descriptions are published (see e.g. [32–36]).

2.1.2 The string model

The piano string is well approximated by a one-dimensional system, described by the wave equation for transversal displacements

$$F_s + T_s \cdot \frac{\partial^2 u_s}{\partial x^2} = \lambda_s \cdot \frac{\partial u_s}{\partial t} + \mu_s \cdot \frac{\partial^2 u_s}{\partial t^2}, \tag{2}$$

where F_s is the excitation force acting on string (because of the force continuity it equals F_h), T_s is the longitudinal tension in string, λ_s is the damping coefficient, μ_s is the string mass per unite length and u_s is the transversal string displacement.

In the current study, piano strings are modelled using the digital waveguide method. The method is based on d'Alembert's solution: the propagating waves are formulated as the sum of opposite directed half-waves

$$u_s(x,t) = u_s^+(ct - x) + u_s^-(ct + x), \tag{3}$$

where c is the vibration propagation velocity and + and − denote the half-waves. The discretization of Eq. (3) is straightforward and can be found in detail in [30, 37].

The original formulation is not suitable to model the hammer-string interaction, because it is known that in the point of impact the resulting displacement is incorrect. Bank dealt with that phenomenon and proposed a delayed force input model (Fig. 1) [31].

Since piano strings are of finite length and clamped on both ends, losses along the string and reflections on terminations have to be modelled. In the case of digital

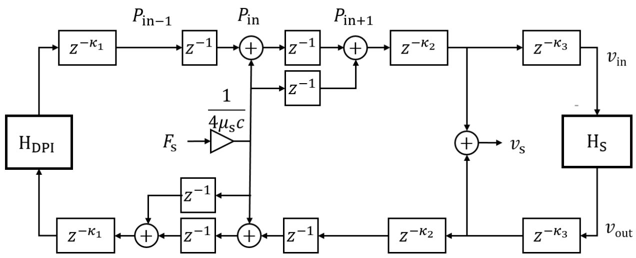

Fig. 1 One-string-waveguide with filters

waveguides all these effects are concentrated in terminations, which are realized through fitted filter sets. In the current study all soundboard-connected effects are modelled in one termination (marked as H_S) and remaining ones (damping, pitch-correction, inharmonicity) are combined in the other one (marked as H_{DPI}). The soundboard filters can be designed based on the modal description of the soundboard, namely on mode shapes (Φ), eigenfrequencies (ω_r), modal masses (m_r) and modal damping coefficients (ξ_r) [38].

2.1.3 Sound radiation

Since the weak sound of the strings are amplified by the soundboard, the sound radiation model is based on the soundboard model. In the case of modeling of near field sound radiation Rayleigh's integral is a practical choice. For the analytical solution the soundboard is embedded in a hypothetic infinite perfectly rigid plate, so each point of the radiator can be considered as a monopole. The required sound pressure function for arbitrary position in the near field ($P(y,\omega)$) is the superposition of the pressure field of these monopoles of area dS

$$P(y,\omega) = \frac{j\omega \cdot \rho_0}{2\pi} \cdot \int_S V(x,\omega) \cdot \frac{e^{-jk|y-x|}}{y-x} \cdot \mathrm{d}S. \tag{4}$$

The normal component of the soundboard velocity ($V(y,\omega)$) can be derived from the modal description of the soundboard. As a result, the transfer function forms a FIR-filter set of the size of the used soundboard modes.

2.2 The soundboard model

2.2.1 Mechanical properties

Wood is mostly described as an orthotropic material: "The longitudinal axis is parallel to the fiber (grain); the radial axis is normal to the growth rings (perpendicular to the grain in the radial direction); and the tangential axis is perpendicular to the grain but tangent to the growth rings." ([18]:p.5-1). High quality piano soundboards are made of spruce (especially Sitka or Norway spruce). The typical mechanical parameters (density ρ, Young's moduli E_i, Poisson's ratio v_{ij} and shear moduli G_{ij}) for spruce occur within the ranges shown in Table 1 ([10, 18, 27, 28]).

2.2.2 The material matrix

The material model is based on the generalized Hooke's law

$$\hat{\sigma}_{ij} = \sum_{k=1}^{3}\sum_{l=1}^{3} \hat{D}_{ijkl} \cdot \hat{\varepsilon}_{kl}, \tag{5}$$

where $\hat{\sigma}_{ij}$ stands for elements of the stress tensor ($[\hat{\sigma}]$), $\hat{\varepsilon}_{ij}$ for the strain tensor and $\hat{D}_{ijkl}$ are the elements of the material tensor. The symmetry of the stress and strain tensors implies that the Voigt matrix notation can be applied, where the material tensor is reduced to a 6 × 6 symmetric matrix $\hat{\boldsymbol{D}}$. The elements of the material matrix can be derived from mechanical properties (E_i, v_{ij}, G_{ij}) and it is well documented in the literature. To determine the applied material matrix ($\boldsymbol{D}$) a transformation from material basis to the reference basis of the geometry must be performed.

To determine forces and moments, the material matrix should be reordered to represent separate groups of membrane ($\boldsymbol{m}$ for 1, 2, 6 indices) and transverse shear ($\boldsymbol{s}$ for 3, 4, 5 indices) stiffnesses. The resulting material matrix has the form of a 2 × 2 block-matrix with symmetric sub-matrices ($\boldsymbol{D}^m$ and $\boldsymbol{D}^s$) of size 3 × 3 in the diagonal and zeros in the anti-diagonal:

$$\boldsymbol{D}^{ms} = \begin{pmatrix} \boldsymbol{D}^m & 0 \\ 0 & \boldsymbol{D}^s \end{pmatrix}. \tag{6}$$

2.2.3 The displacement equation

The dynamics of a general elastic volume (Ω), given by arbitrary boundary (Γ), made from a general Kelvin-Voigt material, is given by the differential equation (balance of linear momentum)

$$\left(\boldsymbol{\mathcal{S}}^{ms}\right)^{\mathrm{T}} \cdot \sigma^{ms} + \boldsymbol{b} = \rho \cdot \frac{\partial^2 \boldsymbol{u}}{\partial t^2}, \tag{7}$$

Table 1 Typical mechanical properties of spruce

Property	Metric	Min.	Max.	Model
ρ	kg m^{-3}	380	460	380
E_1	GPa	10	16	11
E_2	GPa	0.47	0.9	0.65
v_{12}	1	0.26	0.44	0.26
G_{12}	GPa	0.66	1.2	0.66
G_{23}	GPa	3.9	4.2	-

in which $\left(\boldsymbol{\mathcal{S}}^{ms}\right)^{\mathrm{T}} \cdot \boldsymbol{\sigma}^{ms}$ $\left(\boldsymbol{\sigma}^{ms} = \boldsymbol{D}^{ms} \cdot \varepsilon_t^{ms} + \boldsymbol{\mathcal{H}} \cdot \frac{\partial \varepsilon_t^{ms}}{\partial t}\right)$ is the divergence of the stress vector applying frequency-dependent damping matrix $\boldsymbol{\mathcal{H}}$, $\boldsymbol{b}$ contains the body forces, ρ is the density and $\boldsymbol{u}$ describes the displacement of the volume [39].

In the specific case of piano soundboard, the volume is a finite thin plate holding ribs on one side and the bridges on the other one. Assuming that the displacement of the board ($\boldsymbol{u}$) is based on the Kirchhoff-Love theorem, the displacement equation can be rewritten in the form

$$\left(\boldsymbol{\mathcal{S}}^{ms}\right)^{\mathrm{T}} + \boldsymbol{D}^{ms} \cdot \boldsymbol{\mathcal{S}}^{ms} \cdot \boldsymbol{u} + \boldsymbol{\mathcal{H}} \cdot \frac{\partial \boldsymbol{u}}{\partial t} + \boldsymbol{b} = \rho \cdot \frac{\partial^2 \boldsymbol{u}}{\partial t^2}. \tag{8}$$

The goal is to solve the weak formulation of Eq. (8) through discretization of the geometry and function space. To discretization the finite element method is used: the given volume is split into elements, and the solution for displacement equation is approximated by superposition of finite number of polynomial base function ($\boldsymbol{\mathcal{N}}$). Outputs of the finite element representation are the so-called mass and stiffness matrices ($\boldsymbol{\mathcal{M}}$, $\boldsymbol{\mathcal{K}}$) [39].

The damping coefficient in matrix $\boldsymbol{\mathcal{H}}$ are of engineering appraisals or (based on Rayleigh's method) the linear combination of mass- and stiffness matrices [40, 41]. To reduce the size of the resulting matrices, the master-slave multi-freedom constraint theory can be applied: the plate can be handled as master geometry, the ribs and bridges as slave geometries.

2.2.4 The modal description

To determine the modal description, we use the differential equation equivalent to the week formulation of Eq. (8)

$$\boldsymbol{\mathcal{K}} \cdot u(\boldsymbol{x},t) + \boldsymbol{\mathcal{H}} \cdot \frac{\partial u(\boldsymbol{x},t)}{\partial t} + \boldsymbol{\mathcal{M}} \cdot \frac{\partial^2 u(\boldsymbol{x},t)}{\partial t^2} = f(\boldsymbol{x},t). \tag{9}$$

in which $u(\boldsymbol{x},t)$ marks the space and time dependent displacement. Since the modes are free vibrations the damping matrix and the external force f is all zeros. After some algebraic modifications and transformation to frequency domain, the modal description (eigenfrequencies (ω_k) and mode shapes (Φ_k)) can be determined by solving a generalized eigenvalue problem:

$$\left(\boldsymbol{\mathcal{K}} - \omega^2 \cdot \boldsymbol{\mathcal{M}}\right) \cdot U(\boldsymbol{x},\omega) = 0. \tag{10}$$

Arbitrary displacement of the board can be approximated by linear combination, in which mode shapes and modal weights form the required base

$$U(\boldsymbol{x},\omega) = \sum_{k=1}^{n} \Phi_k(\boldsymbol{x}) \cdot \mathfrak{A}_k(\omega). \tag{11}$$

Based on Eq. (16) also the time-dependent displacement for arbitrary excitation can be determined, and so the coupled vibration of strings, and the characteristics of the radiated near field sound.

In practice the mode shapes are chosen such that the modal mass matrix $\boldsymbol{M} = \Phi^{\mathrm{T}} \cdot \boldsymbol{\mathcal{M}} \cdot \Phi$ equals identity and the modal stiffness matrix $\boldsymbol{K} = \Phi^{\mathrm{T}} \cdot \boldsymbol{\mathcal{K}} \cdot \Phi$ is diagonal. The modal damping matrix $\boldsymbol{H} = \Phi^{\mathrm{T}} \cdot \boldsymbol{\mathcal{H}} \cdot \Phi$ in case of Rayleigh's method will also be diagonal, otherwise diagonalization methods are widely in use [42].

3 Numerical example

The model output is demonstrated on a grand piano like geometry (Fig. 2) applying mean extent values based mostly on [9]. The board has a uniform thickness of 8 mm. Bridges are 3 cm wide and of 3 and 1.75 cm high for bass and treble bridges, respectively. Ribs are 2.5 cm wide. Their height varies from 0.5 cm near the edge to 3 cm near their mid-section. For material properties applied in current model see in Table 1 (last column).

The finite element model of the board is represented by 2D triangle plate elements, while the bridges and ribs are modelled using 1D beam elements. The average edge size is 5 mm. Displacements of ribs and bridges are interpolated on the triangular mesh using master-slave multi-freedom constraints.

The modal damping coefficient of the soundboard is set to constant 8% [41], and is considered to be homogenously distributed overall the geometry [43].

One string (MIDI60 ≡ C4 ≡ 261.63 Hz) is attached to the defined soundboard. The string and hammer parameters are estimated based on [27]. The string loss factors are set based on Wograms T20 measurements published in [44]. The initial hammer velocity is set to 1 m/s. The listening position is set to 25 cm distance from the soundboard.

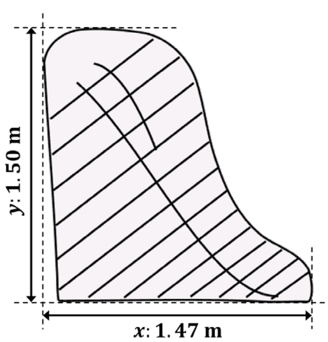

Fig. 2 Example geometry

In the case of soundboard modeling the question of boundary condition is widely discussed, since the special condition of the soundboard glued to the rim. It is supposed that a complex combination of generally used simply supported and clamped condition would be able to model the behavior more properly without modeling the geometry of the rim [7, 45, 46]. For current study the first 1000 eigenfrequencies are computed. For the clamped case the lowest eigenfrequency is at 64 Hz. (Because of the use of modal superposition, the values in the analysis are supposed to be valid up to about 4 kHz.) As expected, the mode density slightly increases for the higher order modes. On the mode shapes (Fig. 3) the stiffening effect of the bridges (in the middle: displacement mostly on both side of the bridges) and ribs (on the right: displacement mostly among ribs) is observable. When the boundary condition is modified to simply supported the eigenfrequencies are shifted downward (by 20 Hz Fig. 4).

It is known that in piano soundboard manufacturing ribs are aligned perpendicular to the board fiber direction (90°). It is very important, not only because of the static properties of the soundboard, but of the modal behavior as well. In the hypothetical case, when ribs are removed, the first eigenfrequency is shifted downward (by 40 Hz), in accordance with the dominance of the stiffeners. Analyzing the results of several numerical simulations it can also be assumed that the modal frequencies decrease for higher-order modes, when the stiffener-fiber angle is adjusted. This effect is independent from the boundary shape and original rib placement. The soundboard is least stiff in the case, when this relative angle is 0°. In this case the overall change in eigenfrequencies is approximately twice as for setting the boundary condition to simply supported, and a bit more than the half as for removing of ribs (bare board Fig. 4). For lower modes the effect of adjustment depends on soundboard shape and rib orientation, the first few eigenfrequencies can even increase.

The computed mode shapes and the bridge position of the selected string affect the computed point admittance heavily. The peaks and valleys of the admittance curve are related to the deviations and quasi stationary parts of the mode shapes and their frequencies. For frequencies with larger peaks, more energy is dissipated by soundboard deformations (Fig. 5). For lower modes this effect is much larger. For higher order modes the curve will be flatter. The cut-off is determined by the frequency, up to which the modal behavior is numerically computed. The characteristic of the computed curve is in quite good match with published measurements for quasi-identical position and soundboard [7].

The radiated sound pressure pattern is as expected (Fig. 6): at the initial part of the pressure-time history the effect of hammer strike is observable (prompt sound: quick rise and fast decay in attack part), then it fades away more slowly (after sound: sustain part [44]). The velocity and decay pattern, as well as the amplitude of the attack depends on the modal behavior of the soundboard, on the bridge position, on the coupling among strings and on the listening position in the room.

In the following paragraphs the radiated sound will be analyzed using some standard descriptors. To be able to compare different soundboards and the effect of their modifications on the radiated sound, quantitative indicators are introduced. A collection of possible indicators is listed e.g. in [47].

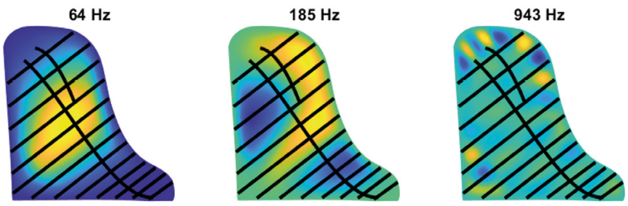

Fig. 3 Example modes

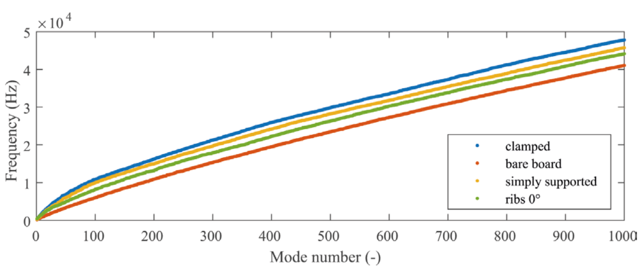

Fig. 4 Eigenfrequencies for different soundboards

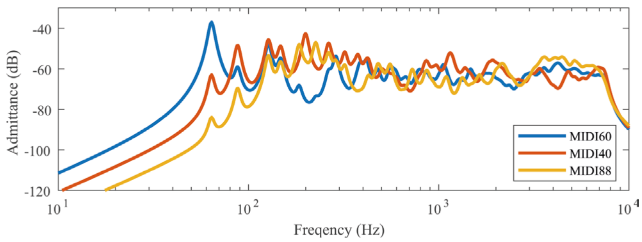

Fig. 5 Admittance for different bridge positions (clamped boundary)

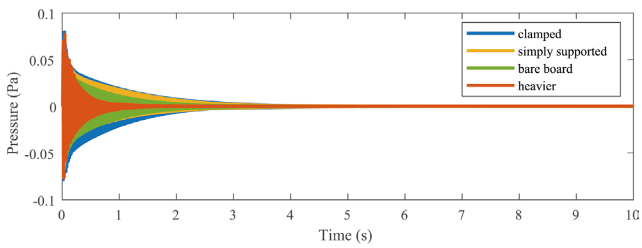

Fig. 6 Sound pressure MIDI60 for different soundboards

Coloring depends on spectral components of the radiated sound. These components can be classified in a harmonic part determined by the strings (fundamental frequency and overtones) and in peaks caused by the modal behavior of the soundboard. The ratio of the harmonic part over total energy is a possible descriptor (harmonic ratio). On the spectrum the string harmonics are dominant, but the effect of the soundboard modal behavior can also be observed clearly (Fig. 7). It is known that besides the fundamental frequency the first five harmonics characterize mostly the piano tone [41], so it is worth concentrating on these. In case of the same strike (same input conditions at the start of our model), soundboards can differently amplify the same frequency range. In the specific loudness diagram, that visualizes the loudness of spectrum components over the whole simulation, this effect is observable, and the first few harmonics seem to play a dominant role in the radiated sound.

Coloring changes over time, because of the different intensity, duration and decay of the harmonics. The dominant harmonics and their ratio to total energy determine how natural and pleasing the tone will be. Spectral flux defines the temporal variation of the spectrum along time and spectral centroid, spread and slope are considered as important parameters of timbre characterization [47, 48]. These indicators are the barycenter of the spectrum, its variance and the amount of decrease of the spectral amplitude.

For the current numerical simulations, it can be assumed that the harmonic ratio increases over 0.9 at about 0.5 s and begins to fall after 5 s depending on the overall decay of the sound for a given soundboard (Fig. 8).

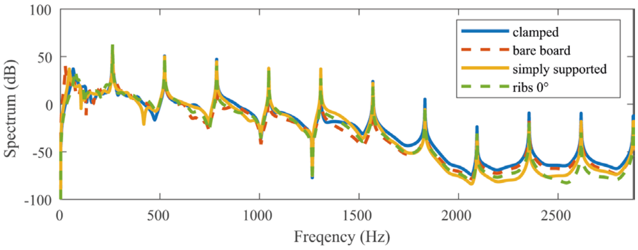

(a)

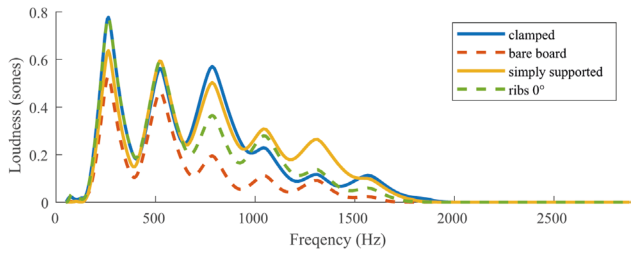

(b)

Fig. 7 Radiated sound spectrum (a) and specific loudness (b) MIDI60 for different soundboards

So, the harmonic character can be considered independent of adjusting the soundboard within reasonable limits. Based on spectral flux, the spectrum is stable over time (Fig. 9), and the spectral slope shows quite good match with the sound pressure function (Figs. 6 and 10).

Examining the decay pattern of harmonic components, one can see that there is a close relationship between the admittance and harmonic decay: for frequencies where the board mobility is higher the harmonic components decay faster (Fig. 11). So, the spectral descriptors and their variation over time is determined directly by the point mobility. It is why, when the listening position is shifted the specific loudness of the sound is changed a bit, but the decay velocity of the harmonic components and so the spectral centroid, flux and slope (for long-term) remain unchanged. The sound pressure level of harmonics at the beginning differs, but the spectral centroid for long-term goes to the same value. On the contrary changing the position of the string along the bridge can cause a significant change in the admittance curve (as extreme case Fig. 5) and so in spectral components of the radiated sound. Likewise, the different boundary conditions and material properties can affect the results heavily through the point mobility.

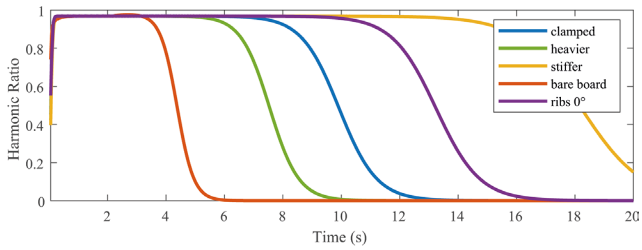

Fig. 8 Harmonic ratio for different soundboards

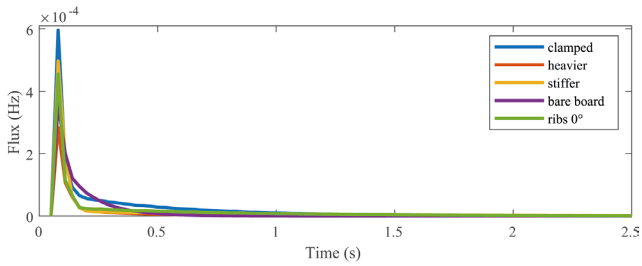

Fig. 9 Spectral flux for different soundboards

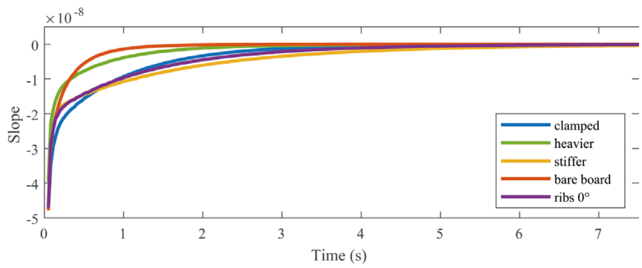

Fig. 10 Spectral slope for different soundboards

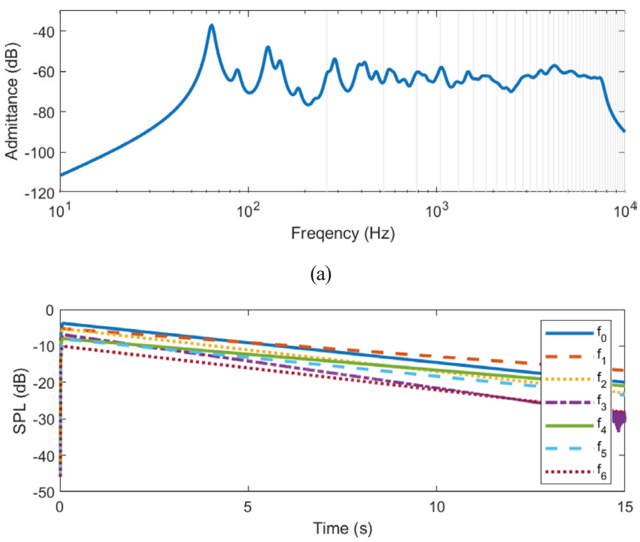

(a)

(b)

Fig. 11 Point mobility on bridge in position MIDI60 with harmonic components (grey lines) of MIDI60 string (a), and Decay of their harmonic components clamped board (b)

In the literature there are numerous parameter sets published to describe the mechanical properties of soundboard wood (in our case spruce). The variance can be explained by the natural diversity of wood samples and the different environmental conditions. It is worth examining the effect of parameter setting.

In first case the soundboard is set to heavier increasing the density from 380 kg/m^3 to another valid value of 460 kg/m^3. As expected, the eigenfrequencies are shifted downward systematically. The fundamental frequency and the first harmonic decay double so fast as in original case. But e.g. the third harmonic decays much slower and becomes dominant in the long term. That can be seen also in spectral centroid (Fig. 12).

If the soundboard is made from stiffer material (longitudinal Young's modulus set to 16 GPa from 11 GPa) the eigenfrequencies (and so the admittance curve) are shifted upward. Because of the modification of the admittance curve in this case the fundamental frequency decays much slower and stays dominant over harmonics in time.

The differences in spectral damping (Fig. 11) or in spectral centroid over time (Fig. 12) can also be clearly

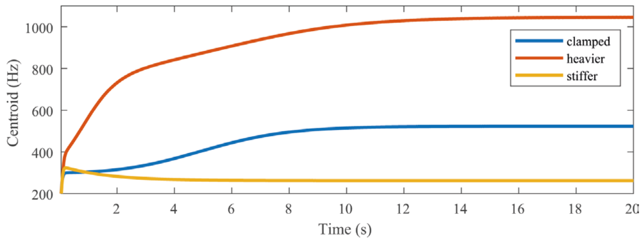

Fig. 12 Spectral centroid for different soundboard materials

noticed in the sound samples, as they will be more or less bright by time.

4 Conclusion

A simplified 2D piano model was introduced from strike to sound radiation. Instead of dealing only with the modal behavior of the soundboard, or with the softly defined quality of the piano tone, the near field radiated sound for different soundboards was compared using standard quantitative indicators.

It was shown that the modal behavior, positions and eigenfrequencies of strings determine the characteristics of the near field radiated sound, while modal behavior depends on the geometry, boundary condition and selected material parameters. The effect of modification of these parameters was discussed.

The presented simulation results show that although the stiffening effect of ribs can be considered as dominant, the effect of the fiber orientation of the board cannot be neglected completely. The effect of fiber direction on the eigenfrequencies is of similar magnitude as e.g., changing the boundary condition from clamped to simply supported.

The admittance is related to the modal behavior and determines the calculated sound parameters directly, so the descriptors of the sound quality can show huge differences for different string positions, even for the same string and soundboard combination.

Based on current simulations wooden soundboards result in harmonic radiated sounds even for large modifications in the initial mechanical descriptors of the applied material.

It was shown that although the harmonic decay velocities are independent from the listening position, the loudness and so the perceived sound can differ significantly.

References

[1] Bank, B., Chabassier, J. "Model-Based Digital Pianos: From Physics to Sound Synthesis", IEEE Signal Processing Magazine, 36(1), pp. 103–114, 2019. https://doi.org/10.1109/MSP.2018.2872349

[2] Elie, B., Boutillon, X., Chabassier, J., Ege, K., Laulagnet, B., Trévisan, B., Cotté, B., Chauvat, N. "MAESSTRO: A sound synthesis framework for Computer-Aided Design of piano soundboards", In: Proceedings of ISMA 2019 International Symposium on Musical Acoustics, Detmold, Germany, 2019, pp. 359–366. ISBN 978-3-939296-16-4

[3] Bilhuber, P. H., Johnson, C. A. "The influence of the soundboard on piano tone quality", The Journal of the Acoustical Society of America, 11(3), pp. 311–320, 1940. https://doi.org/10.1121/1.1916039

[4] Giordano, N. "Mechanical impedance of a piano soundboard", The Journal of the Acoustical Society of America, 103(4), pp. 2128–2133, 1998. https://doi.org/10.1121/1.421358

[5] Berthaut, J., Ichchou, M. N., Jézéquel, L. "Piano soundboard: structural behavior, numerical and experimental study in the modal range", Applied Acoustics, 64(11), pp. 1113–1136, 2003. https://doi.org/10.1016/S0003-682X(03)00065-3

[6] Corradi, R., Fazioli, P., Marforio, S., Paluello, A., Ripamonti, F., Squicciarini, G. "Modal analysis of a grand piano soundboard", In: Proceedings of ISMA2010 including USD2010, Leuven, Belgium, 2010, pp. 59–72. ISBN 9789073802872

[7] Corradi, R., Miccoli, S., Squicciarini, G., Fazioli, P. "Modal analysis of a grand piano soundboard at successive manufacturing stages", Applied Acoustics, 125, pp. 113–127, 2017. https://doi.org/10.1016/j.apacoust.2017.04.010

[8] Bank, B., Zambon, S., Fontana, F. "A modal-based real-time piano synthesizer", IEEE Transactions on Audio, Speech, and Language Processing, 18(4), pp. 809–821, 2010. https://doi.org/10.1109/TASL.2010.2040524

[9] Ege, K. "La table d'harmonie du piano - Études modales en basses et moyennes fréquences" (The piano soundboard – Modal studies in the low- and the mid-frequency range), PhD Thesis, Ecole Polytechnique, 2009. (in French)

[10] Boutillon, X., Ege, K. "Vibroacoustics of the piano soundboard: Reduced models, mobility synthesis, and acoustical radiation regime", Journal of Sound and Vibration, 332(18), pp. 4261–4279, 2013. https://doi.org/10.1016/j.jsv.2013.03.015

[11] Ege, K., Boutillon, X. "Synthetic description of the piano soundboard mechanical mobility", In: Proceedings of 20th International Congress on Acoustics, ICA 2010, Sydney, Australia, 2010, 427. ISBN 978-0-646-54052-8

[12] Ege, K., Boutillon, X. "Global and local synthetic descriptions of the piano soundboard", In: Forum Acusticum 2011, Aalborg, Denmark, 2011, pp. 473–478.

[13] Chabassier, J. "Modélisation et simulation numérique d’un piano par modèles physiques" (Modeling and numerical simulation of a piano), PhD Thesis, Ecole Polytechnique, 2012. (in French)

[14] Thompson, D. J., Ferguson, N. S., Yoo, J. W., Rohlfing, J. "Structural waveguide behaviour of a beam–plate system", Journal of Sound and Vibration, 318(1–2), pp. 206–226, 2008. https://doi.org/10.1016/j.jsv.2008.04.011

[15] Dumond, P., Baddour, N. "Can a brace be used to control the frequencies of a plate?", SpringerPlus, 2(1), 558, 2013. https://doi.org/10.1186/2193-1801-2-558

[16] Dumond, P., Baddour, N. "A structured method for the design-for-frequency of a brace-soundboard system using a scalloped brace", Applied Acoustics, 88, pp. 96–103, 2015. https://doi.org/10.1016/j.apacoust.2014.08.004

[17] Trévisan, B., Ege, K., Laulagnet, B. "Prediction of orthotropic ribbed plates' vibro-acoustics mechanisms: application to the piano soundboard", In: International Symposium on Musical Acoustics, ISMA 2014, Le Mans, France, 2014, ISMA2014/40.

[18] Ross, R. J. "Wood handbook: wood as an engineering material", U.S. Department of Agriculture, Forest Service, Forest Products Laboratory, Madison, WI, USA, Rep. FPL-GTR-190, 2010. https://doi.org/10.2737/FPL-GTR-190

[19] Persson, K. "Micromechanical Modelling of Wood and Fibre Properties", PhD Thesis, Lund University, 2000.

[20] Tabet, T. A., Aziz, F. A. "Cellulose microfibril angle in wood and its dynamic mechanical significance", In: van de Ven, T., Godbout, L. (eds.) Cellulose - Fundamental Aspects, IntechOpen, 2013, pp. 113–142. ISBN 978-953-51-1183-2 https://doi.org/10.5772/51105

[21] Ono, T. "Frequency responses of wood for musical instruments in relation to the vibrational properties", Journal of the Acoustical Society of Japan (E), 17(4), pp. 183–193, 1996. https://doi.org/10.1250/ast.17.183

[22] Hilde, C., Woodward, R., Avramidis, S., Hartley, I. D. "The acoustic properties of water submerged lodgepole pine (*Pinus contorta*) and spruce (*Picea* spp.) wood and their suitability for use as musical instruments", Materials, 7(8), pp. 5688–5699, 2014. https://doi.org/10.3390/ma7085688

[23] Wegst, U. G. K. "Wood for sound", American Journal of Botany, 93(10), pp. 1439–1448, 2006. https://doi.org/10.3732/ajb.93.10.1439

[24] Yoshikawa, S. "Acoustical classification of woods for string instruments", The Journal of the Acoustical Society of America, 122(1), pp. 568–573, 2007. https://doi.org/10.1121/1.2743162

[25] Brémaud, I. "Acoustical properties of wood in string instruments soundboards and tuned idiophones: Biological and cultural diversity", The Journal of the Acoustical Society of America, 131(1), pp. 807–818, 2012. https://doi.org/10.1121/1.3651233

[26] Bennett, B. C. "The sound of trees: Wood selection in guitars and other chordophones", Economic Botany, 70(1), pp. 49–63, 2016. https://doi.org/10.1007/s12231-016-9336-0

[27] Chabassier, J., Duruflé, M. "Physical parameters for piano modeling", Inria, Talence, France, Rep. RT-0425, 2012.

[28] Trévisan, B., Ege, K., Laulagnet, B. "A modal approach to piano soundboard vibroacoustic behavior", The Journal of the Acoustical Society of America, 141(2), pp. 690–709, 2017. https://doi.org/10.1121/1.4974860

[29] Arz, J.-P., Laville, F. "Experimental characterization of small thickness elastomeric layers submitted to impact loading", Journal of Sound and Vibration, 326(1–2), pp. 302–313, 2009. https://doi.org/10.1016/j.jsv.2009.04.033

[30] Smith III, J. O. "Efficient synthesis of stringed musical instruments", In: Opening a New Horizon: Proceedings of the 1993 International Computer Music Conference, Tokyo, Japan, 1993, pp. 64–71.

[31] Bank, B. "Physics-based sound synthesis of the piano", MSc Thesis, Budapest University of Technology and Economics, Published as Report 54 of Helsinki University of Technology, Laboratory of Acoustics and Audio Signal Processing, 2000. ISBN 951-22-5037-3

[32] Stulov, A. "Hysteretic model of the grand piano hammer felt", The Journal of the Acoustical Society of America, 97(4), pp. 2577–2585, 1995. https://doi.org/10.1121/1.411912

[33] Stulov, A. "Dynamic behavior and mechanical features of wool felt", Acta Mechanica, 169(1–4), pp. 13–21, 2004. https://doi.org/10.1007/s00707-004-0104-3

[34] Avanzini, F., Rocchesso, D. "Modeling collision sounds: Non-linear contact force", In: Proceedings of the COST G-6 Conference on Digital Audio Effects (DAFX-01), Limerick, Ireland, 2001, pp. 61–66.

[35] Bensa, J., Gibaudan, F., Jensen, K., Kronland-Martinet, R. "Note and hammer velocity dependence of a piano string model based on coupled digital waveguides", In: Proceedings of the 2001 International Computer Music Conference, ICMC 2001, Havana, Cuba, pp. 95–98, 2001.

[36] Giordano, N., Millis, J. P. "Using physical modeling to learn about the piano: New insights into the hammer-string force", In: Proceedings of ICA 2004: the 18th International Congress on Acoustics, Kyoto, Japan, 2004, pp. 2113–2116. ISBN 9784990191511

[37] Smith, J. O. "Physical modeling using digital waveguides", Computer Music Journal, 16(4), pp. 74–91, 1992. https://doi.org/10.2307/3680470

[38] Bank, B., Karjalainen, M. "Passive admittance synthesis for sound synthesis applications", In: Acoustics'08, Paris, France, 2008, pp. 3901–3906. ISBN 9782952110549

[39] Zienkiewicz, O. C., Taylor, R. L. "The Finite Element Method for Solid and Structural Mechanics", Elsevier, 2005. ISBN 9780750663212

[40] Zabaras, N., Pervez, T. "Viscous damping approximation of laminated anisotropic composite plates using the finite element method", Computer Methods in Applied Mechanics and Engineering, 81(3), pp. 291–316, 1990. https://doi.org/10.1016/0045-7825(90)90058-T

[41] Göken, J., Fayed, S., Schäfer, H., Enzenauer, J. "A study on the correlation between wood moisture and the damping behaviour of the tonewood spruce", Acta Physica Polonica A, 133(5), pp. 1241–1260, 2018. https://doi.org/10.12693/aphyspola.133.1241

[42] Felippa, C. A., Guo, Q., Park, K. C. "Mass matrix templates: General description and 1D examples", Archives of Computational Methods in Engineering, 22(1), pp. 1–65, 2015. https://doi.org/10.1007/s11831-014-9108-x

[43] Unruh, O. "Influence of inhomogeneous damping distribution on sound radiation properties of complex vibration modes in rectangular plates", Journal of Sound and Vibration, 377, pp. 169–184. 2016. https://doi.org/10.1016/j.jsv.2016.05.009

[44] Askenfelt, A. "Five lectures on the acoustics of the piano", Royal Swedish Academy of Music, Stockholm, 1990. ISBN 9789185428625

[45] Keane, M. "An Evaluation of Piano Sound and Vibration Leading to Improvements Through Modification of the Material Properties of the Structure", PhD Thesis, University of Auckland, 2006.

[46] Borland, M. "The characterization of piano soundboard materials with respect to their vibrational and psychoacoustical properties for evaluation purposes", PhD Thesis, University of Waterloo, 2010.

[47] Peeters, G. "A large set of audio features for sound description (similarity and classification) in the CUIDADO project", Ircam, Paris, France, 2004.

[48] Marozeau, J., de Cheveigné, A., McAdams, S., Winsberg, S. "The dependency of timbre on fundamental frequency", The Journal of the Acoustical Society of America, 114(5), pp. 2946–2957, 2003. https://doi.org/10.1121/1.1618239